MIMO Ad Hoc Networks: Medium Access Control, Saturation Throughput, and Optimal Hop Distance

Ming Hu and Junshan Zhang

Abstract: **In this paper, we explore the utility of recently discovered multiple-antenna techniques (namely MIMO techniques) for medium access control (MAC) design and routing in mobile ad hoc networks. Specifically, we focus on ad hoc networks where the spatial diversity technique is used to combat fading and achieve robustness in the presence of user mobility. We first examine the impact of spatial diversity on the MAC design, and devise a MIMO MAC protocol accordingly. We then develop analytical methods to characterize the corresponding saturation throughput for MIMO multi-hop networks. Building on the throughout analysis, we study the impact of MIMO MAC on routing. We characterize the optimal hop distance that minimizes the end-to-end delay in a large network. For completeness, we also study MAC design using directional antennas for the case where the channel has a strong line of sight (LOS) component. Our results show that the spatial diversity technique and the directional antenna technique can enhance the performance of mobile ad hoc networks significantly.**

Index Terms: **Ad hoc networks, hop distance, medium access control, MIMO, saturation throughput, spatial diversity.**

I. INTRODUCTION

The past few years have witnessed a surge of interest in wireless ad hoc networks that can facilitate communications between wireless devices, without using a planned infrastructure. A central issue in mobile ad hoc networks (MANET) is mobility. In particular, due to the user mobility, the wireless channels often experience time-varying fading, making the protocol design more challenging. It has recently been shown that in fading channels, using multiple antennas at the wireless transmitter and the receiver, namely the multiple-input multiple-output (MIMO) technique, can boost up the channel capacity significantly [1], [2]. It is envisioned that the MIMO techniques can help to propel significant advances towards robust ad hoc networks. Thus, it is of great importance to leverage the impact of MIMO techniques on the design and the analysis of mobile ad hoc networks.

Unfortunately, there has been little work on MIMO ad hoc networks in the presence of mobility, and it is unclear how to take advantage of MIMO techniques in mobile ad hoc networks. It is well known that for point-to-point communications, a MIMO link can offer spatial multiplexing gain and spatial (antenna) diversity gain [3], [4]. We note that the co-channel interference reduces the number of "effective receive antennas"; as a result, it is challenging to achieve spatial multiplexing gain in an inference-limited environment [3]. That is to say, complicated interference management is needed to harvest spatial multiplexing gains. On the other hand, spatial diversity (including both transmit diversity and receive diversity) can be used to combat fading and improve the reliability of the wireless links (see [5], [6], and [7]), and is particularly useful for MANETs. Thus motivated, we focus on exploiting spatial diversity for medium access control (MAC) design and routing in MANETs.

In this paper, we consider mobile ad hoc networks where the spatial diversity technique is used to combat fading and achieve robustness in the presence of user mobility. In particular, we first exploit spatial diversity for MAC design, and develop new analytical methods to evaluate the corresponding throughput performance. Building on this and the giant stepping notion in [8], we then characterize the optimal hop distance in the sense of minimizing the end-to-end delay in a large network. Simply put, our contributions are three folds. 1) We propose a MIMO MAC scheme with spatial diversity, based on the RTS/CTS mechanism; and this scheme makes use of spatial diversity and multirate transmissions. 2) We analyze the average throughput of mult-hop ad hoc networks using spatial diversity. Specifically, assuming a homogenous ad hoc network, we present an analytical approach to characterize the saturation throughput per user. A key feature that distinguishes our work from [9] is that our method is more general and can be applied to multi-hop ad hoc networks in the presence of fading. 3) We generalize the above cross-layer study to joint consideration of MIMO MAC and routing. In particular, we take a holistic perspective to investigate the impact of MIMO MAC on routing, and characterize the optimal hop distance which minimizes the end-to-end delay in a large multi-hop network. Our results show that the MIMO techniques can enhance the performance of mobile ad hoc networks significantly.

For the sake of completeness, we also study an interesting case—ad hoc networks using directional antennas when the channels have strong line of sight (LOS) components. Note that directional antennas work well only when the LOS components in the channel are strong [10], whereas spatial diversity is used when spatial channels experience more or less independent fading. Specifically, we use a general directional antenna model with both a mainlobe and sidelobes, and propose *directional listening* for the MAC design. One salient feature is that directional listening can resolve the hidden terminal problem due to the asymmetry in antenna gain (see [11] and [12]). Along the lines above, we also characterize the saturation throughput for ad hoc networks using directional antennas.

In related works, [13] proposed a MIMO MAC protocol with spatial multiplexing, assuming closed-loop MIMO and ideal in-

Manuscript received August 1, 2004.

M. Hu is with the Nokia Mobile Phones, San Diego, CA 92131, email: ming.hu@nokia.com.

J. Zhang is with the Department of Electrical Engineering, Arizona State University, Tempe, AZ 85287, email: junshan.zhang@asu.edu.

This research is partially supported by National Science Foundation through the grant ANI-0238550 and by a grant from the Intel Research Council.

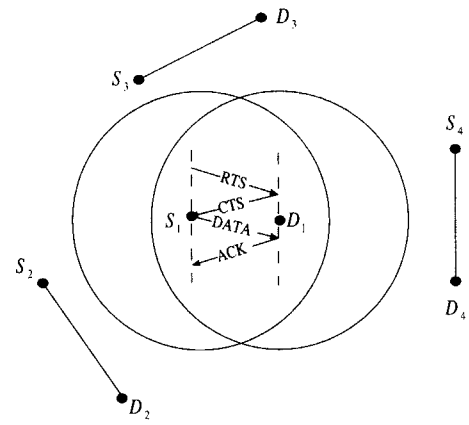

Fig. 1. A simple diagram for RTS/CTS handshaking in IEEE 802.11.

terference cancellation. In [11], the direction of arrival (DOA) information from the directional antennas is incorporated into the MAC, and basic directional MAC (DMAC) and multi-hop RTS MAC (MMAC) are devised accordingly. A similar approach is also developed in [12]. In [14], a receiver-oriented multiple access (ROMA) protocol is introduced to fully utilize the multiple-beam forming capability of antenna arrays. Along a different avenue, much attention has also been paid to find optimal hop distances for multihop networks using ALOHA (e.g., [15], [16], and [17]). Recent work [18] presents an intriguing performance comparison between adaptive MAC working with minimum hop routing and fixed high-rate IEEE 802.11 MAC with minimum hop routing.

The rest of this paper is organized as follows. In the next section, we introduce system models. In Section III, we study the ad hoc networks using spatial diversity. We devise the MIMO MAC protocol and analyze the saturation throughput accordingly. In Section IV, we study joint consideration of MIMO MAC and routing, and characterize the optimal hop distance in the presence of fading. In Section V ,we address the MAC protocol and the saturation throughput analysis for ad hoc networks using directional antennas. The conclusions are given in Section VI.

II. SYSTEM MODELS

A. Channel Model

In wireless communications, due to the user mobility or the variations in the propagation environments, there exhibits time-varying fading. Simply put, in a fading channel, the channel gain can be expressed as

$$h = ae^{j\phi} + b, \tag{1}$$

where $ae^{j\phi}$ denotes the LOS component and is constant, and b denotes the time-varying component of the fading. In mobile ad hoc networks, when the LOS component is very weak, the channel can be well modeled by Rayleigh fading.

Consider an ad hoc network where each node is equipped with an M-element antenna array. Suppose there are K_s active source-destination (S-D) pairs $\{S_k, D_k\}$, $k = 1, \cdots, K_s$. The active communication links are established via the RTS/CTS dialogue, as is shown in Fig. 1. Without loss of generality, consider the link corresponding to the pair $\{S_1, D_1\}$. The received signal at node D_1 is

Table 1. The Alamouti scheme (2 × 2 spatial diversity).

Tx	Antenna element 1	Antenna element 2
Time t	x_1	x_2
Time t+T	$-x_2^*$	x_1^*

$$\mathbf{y_1} = \sqrt{\frac{P_1}{Md_{1,1}^{\alpha}}}\mathbf{H}_{1,1}\mathbf{x}_1 + \sum_{i=2}^{K_s}\sqrt{\frac{P_i}{Md_{i,1}^{\alpha}}}\mathbf{H}_{i,1}\mathbf{x}_i + \mathbf{v}_1, \tag{2}$$

where for $i = 1, \cdots, K_s$,

- P_i is the total transmission power at transmitter S_i,
- $\mathbf{x}_i$ is the transmitted signal at transmitter S_i, with normalized (average) transmission power at each antenna array to be 1, in each symbol period;
- $d_{i,1}$ is the distance between transmitter S_i and receiver D_1,
- $\mathbf{H}_{i,1}$ is the MIMO channel matrix between transmitter S_i and receiver D_1. We assume that the entries in $\mathbf{H}_{i,1}$ are independently complex circular symmetric Gaussian with unit variance,
- $\mathbf{v}_1$ is the additive white Gaussian noise with i.i.d. entries $v_{i,j} \sim \mathcal{CN}(0,1)$.

B. The Spatial Diversity Concept

Spatial diversity, including both transmit diversity and receive diversity, has recently been studied extensively to improve the reliability of wireless links. A comprehensive review on spatial diversity can be found in [19]. To get a more concrete sense, we use the Alamouti scheme to illustrate the basic idea of spatial diversity. Assume that one transmitter with a two-element antenna uses the transmission scheme shown in Table 1, and the fading coefficient is fixed for two consecutive transmissions. The receiver can estimate the signals by using the following detector [5]:

$$\hat{x}_1 = h_{11}^* r_1(t) + h_{21} r_1^*(t+T) + h_{12}^* r_2(t) + h_{22} r_2^*(t+T) \tag{3}$$

$$\hat{x}_2 = h_{21}^* r_1(t) - h_{11} r_1^*(t+T) + h_{22}^* r_2(t) - h_{21} r_2^*(t+T), \tag{4}$$

where h_{ij} denotes the fading coefficient for the spatial channel from transmit antenna element i to receive antenna element j, and $r_i(t)$ denotes the received signal at receive antenna element i at time t. It follows that

$$\tilde{x}_1 = (|h_{11}|^2 + |h_{12}|^2 + |h_{21}|^2 + |h_{22}|^2)x_1 + \tilde{n}_1 \tag{5}$$

$$\tilde{x}_2 = (|h_{11}|^2 + |h_{12}|^2 + |h_{21}|^2 + |h_{22}|^2)x_2 + \tilde{n}_2, \tag{6}$$

where $\tilde{n}$ denotes the noise. Since the channel coefficient is i.i.d., this estimation achieves maximal ratio combining with a diversity order of 2 × 2, as is shown in (5) and (6). In general, in an ad hoc network where each node has an M-element antenna array, the MIMO systems can yield a maximum diversity order of M^2.

III. MAC DESIGN USING SPATIAL DIVERSITY AND ANALYSIS OF SATURATION THROUGHPUT

A. Spatial Diversity versus Spatial Multiplexing

In mobile communications, spatial multiplexing or spatial diversity can be utilized [5], [7], [19]. Although the trade-offs and relationships between these gains in a single-user MIMO channel are relatively well understood [3], [4], the utility of MIMO techniques in ad hoc networks is still at its infant stage. We strive to make some steps along this direction.

Consider the MIMO signal model presented in Section II. Let $\mathbf{R}_1$ be the covariance matrix of the interference-plus-noise term at Receiver D_1. That is,

$$\mathbf{R}_1 = \mathbf{Q} + \mathbf{I}_M, \tag{7}$$

with

$$\mathbf{Q} = \sum_{i=2}^{K_s} \frac{P_i}{M d_{i,1}^{\alpha}} \mathbf{H}_{i,1}\mathbf{H}_{i,1}^H, \tag{8}$$

where we use the fact that $\mathbb{E}[\mathbf{x}_i\mathbf{x}_i^H] = \mathbf{I}$.

Assume that the channel matrix $H_{1,1}$ is unknown at the transmitter S_1, but is known at the receiver D_1. It is shown that the spatial multiplexing gain is given by $\min(M, N_e)$, where N_e is the number of effective receive antennas, defined as $N_e = M - \text{rank}(\mathbf{Q})$ [3]. In practice, the number of antenna elements in mobile stations cannot be large. It is not difficult to see that $\text{rank}(\mathbf{Q})$ is comparable to M in interference-limited regimes. In light of this, we conclude that to achieve the spatial multiplexing gain, sophisticated interference management schemes are needed. On the other hand, spatial diversity can enhance the link reliability significantly in mobile communications. Thus motivated, we focus on MAC design using spatial diversity, where the spatial degrees of freedom embedded in the MIMO channels are used to improve the link quality and multi-rate transmissions.

B. SD-MAC: Exploiting Spatial Diversity for Medium Access Control

In an ad hoc network where each node has an M-element antenna array, each MIMO system can yield M^2 degrees of freedom for communications [3], [4]. In this paper, we assume space-time block codes [5], [7] are used to achieve the full diversity order M^2. We devise a MAC protocol using spatial diversity, namely SD-MAC, based on the RTS/CTS mechanism of the IEEE 802.11 distributed coordination function (DCF). Building on the IEEE 802.11 DCF, the proposed SD-MAC exhibits the following new features: 1) space-time codes are used for four-way handshaking to achieve full-order spatial diversity; 2) for carrier sensing, if the average interference across antenna elements is higher than the threshold, the channel is determined as busy, and the node has to defer its transmission; and 3) the transmission node adapts the data rate for the DATA packet, according to the channel conditions.

We assume that channel gains are obtained by using preamble symbols. The proposed MAC protocol exploiting spatial diversity, namely SD-MAC, can be outlined as follows.

- *RTS transmission*: The source node, denoted S_k, receives a packet from its upper layer. Then, S_k performs virtual carrier sensing by checking the NAV table. If the NAV table is empty, S_k uses multiple antennas to carry out the physical carrier sensing. If the average interference power across receive antennas is lower than the threshold for a period of DIFS, the channel is regarded as idle, and is available for the transmission. Then, the RTS packet with default (basic) data rate is transmitted by using the spatial diversity technique (e.g., space-time coding). If the NAV table is not empty, or the channel is not sensed idle, the user needs to backoff for a random period and defer its transmission. In particular, the user continues (virtual and physical) carrier sensing, and counts down the backoff counter only if the channel is idle. When the backoff counter becomes zero, the packet is sent out immediately.
- *RTS/CTS listening*: All idle nodes in the neighborhood overhear the RTS/CTS packets. Specifically, each idle node estimates the channels using the preamble symbols, decodes space-time signals, obtains the transmission duration from the header of that packet, and then updates its NAV table.
- *RTS reception and CTS transmission*: The destination node D_k performs virtual and physical carrier sensing, after receiving the RTS packet. If the NAV table is empty and the channel is idle for a duration SIFS, the channel is free. Then, D_k selects the rate control parameters for the following DATA packet from S_k based on the channel estimation, and transmits such information via the default-rate CTS packet to S_k using the spatial diversity technique. Otherwise, the CTS transmission is cancelled.
- *CTS reception and DATA transmission*: After the RTS transmission, the source node S_k waits for the CTS packet. Upon receiving the CTS packet, S_k senses the channel. If the channel is idle for a duration of SIFS, S_k adapts the transmission data rate according to the information from the CTS packet, and transmits the multi-rate DATA packet by using the spatial diversity technique. If the CTS packet does not arrive within a time-out window, S_k would resend the RTS packet.
- *DATA reception and ACK transmission*: After sending out the CTS packet, the node D_k moves to the DATA reception phase. When the DATA packet is completely received, D_k confirms the reception by sending a default-rate ACK packet to S_k.

In summary, the above MAC design utilizes spatial diversity, and is based on the IEEE 802.11 DCF. The proposed SD-MAC takes into account the impact of spatial diversity on overhearing, the RTS/CTS dialogue, and data transmissions.

C. Saturation Throughput: The Spatial Diversity Case

Next, we characterize the throughput of multi-hop MIMO ad hoc networks. We focus on the saturation throughput, which is defined as the maximum load when the system is in saturation conditions [9]. That is, each user always has packets in its buffer waiting for transmission.

In [9], Bianchi studies the saturation throughput of one basic service set (BSS). Recall that in the IEEE 802.11 standards, all users within one BSS can communicate directly with each others. By making use of this property, the saturation throughput

can be obtained by examining the system states of a BSS. In multi-hop ad hoc networks, however, users may not hear each other. Furthermore, different from [9] which assumes a constant data rate, our study focuses on MAC with multi-rate transmissions over fading channels. Therefore, the methods in [9] cannot be applied directly to calculate the saturation throughput for such cases. In the following, based on [9], we develop a new approach to characterize the throughput for multi-hop ad hoc networks.

C.1 Markov Models for The RTS/CTS Mechanism

Along the line of [9], we assume perfect channel sensing in an ad hoc network with the RTS/CTS mechanism, and thus collisions occur only on the RTS frames. Also, the "collision" (loss) probability of each packet p is a constant [9]. Under saturation conditions, the CSMA/CA process can be modeled as a two-dimensional Markov chain, and the probability τ that a station transmits in randomly chosen time slot is given by

$$\tau = \frac{2(1-2p)}{(1-2p)(W+1)+pW(1-(2p)^m)}, \tag{9}$$

where p is the collision probability, W is the minimum backoff window in terms of backoff slots, and m is the maximum backoff stage.

C.2 Saturation Throughput per User

Next, we derive the saturation throughput for a multi-hop network using spatial diversity. We consider a homogeneous ad hoc network, in which the events experienced by one user are statistically the same as those of other users; and "statistically" here refers to long-term statistics. We say that such a user is a *typical user*. We first examine the events experienced by a typical user, and derive the corresponding saturation throughput per user.

In the following, we model the events experienced by a typical user (say S_k) into five states: 1) S_k does not transmit and detects the channel idle; 2) S_k does not transmit and overhears one RTS packet from only one of the neighboring users, as if it "views" that user has a successful transmission; 3) S_k does not transmit and overhears a collision among the transmissions of other users; 4) S_k has a successful transmission; and 5) the transmission of S_k collides with that of the others. Let $\{p_i, i=1,\cdots,5\}$ denote the probabilities corresponding to the above events. Then, the average throughput of a typical user under the saturation condition can be expressed as

$$U = \frac{p_4 \mathbb{E}[L]}{\sum_{i=1}^{5} p_i T_i}, \tag{10}$$

where $\mathbb{E}[L]$ is the average packet payload size, and T_i denotes the duration of state i. Let ϵ denote the duration of a backoff slot, i.e., the minimum time needed for transmission detection, T_s be the average time of a successful transmission, and T_c be the average duration of a collision. It can be shown that $T_1 = \epsilon$, $T_2 = T_4 = T_s$, and $T_3 = T_5 = T_c$. Under the RTS/CTS mechanism, the T_s and T_c are given by

$$\begin{aligned} T_s =& RTS + SIFS + \delta + CTS + SIFS + \delta + OH \\ &+ \mathbb{E}[T_p] + SIFS + \delta + ACK + DIFS + \delta, \end{aligned} \tag{11}$$

$$T_c = RTS + DIFS + \delta, \tag{12}$$

where δ is the propagation delay, OH is the overhead including both MAC and PHY headers, and $\mathbb{E}[T_p]$ is the average transmission duration for payload. Note that although the states of one user depend on those of the others, each user has a statistically identical (renewal) period $\sum_{i=1}^{5} p_i T_i$, and hence the same average throughput. Moreover, the successful transmitted packets of one user does not overlap with others. Therefore, the total average throughput in the area with K users can be shown to be KU.

We now derive the saturation throughput for the MIMO ad hoc networks with spatial diversity. We first establish another relationship between τ and p. Worth pointing out is that p denotes the probability that the RTS packet cannot be received correctly. Since fading can also cause the loss of the RTS packet, in the spatial diversity case, p consists of the probability incurred by both collision and fading. Let p_c denote the packet loss probability that is due to collisions only, and p_f denote the packet loss probability due to fading.

Assume there are K_a users within the coverage of each node. K_a can be approximated as $K_a = \pi A^2 \rho$, where A is the coverage range, and ρ is the node density. Suppose that the distance r between any two nodes obeys a distribution with probability density function (pdf) $f_r(r)$. Then, the average packet loss probability due to fading can be expressed as

$$p_f = \int_r p_f(r) f_r(r) dr, \tag{13}$$

where $p_f(r)$ is the loss probability due to fading, for a given distance r. The probability of the packet loss due to collisions can then be calculated as

$$\begin{aligned} p_c &= (1-p_f)\Big[1-(1-\tau)\Big((1-\tau)^{K_a-2} + \\ &\quad \binom{K_a-2}{1}(1-\tau)^{K_a-3}\tau p_f + \cdots + (\tau p_f)^{K_a-2}\Big)\Big] \\ &= (1-p_f)\Big[1-(1-\tau)(1-\tau+\tau p_f)^{K_a-2}\Big]. \end{aligned} \tag{14}$$

Therefore, the loss probability of the RTS packet is given by

$$p = p_c + p_f = (1-p_f)\Big[1-(1-\tau)(1-\tau+\tau p_f)^{K_a-2}\Big] + p_f. \tag{15}$$

Combining (9) and (15), τ and p can be obtained by numerical methods.

Next, we characterize the state probabilities as follows.

p_1 : S_k is listening, and it detects the channel to be empty:

$$p_1 = (1-\tau)(1-\tau+\tau p_f)^{K_a-1}. \tag{16}$$

p_2 : S_k is listening, and hears a handshaking packet from one of its neighbors:

$$p_2 = (1-\tau)(K_a-1)(1-p_f)\tau(1-\tau+\tau p_f)^{K_a-2}. \tag{17}$$

p_3 : S_k is listening, and detects a "collision" among the transmissions of its neighbors:

$$\begin{aligned} p_3 = (1-\tau)[1-(1-\tau+\tau p_f)^{K_a-1} \\ -(K_a-1)(1-p_f)\tau(1-\tau+\tau p_f)^{K_a-2}]. \end{aligned} \tag{18}$$

Table 2. System parameters in ad hoc networks.

Propagation delay	1 μs
SIFS	10 μs
DIFS	50 μs
Backoff slot	20 μs
MAC header	272 bits
PHY header	192 bits
RTS	160 bits + PHY header
CTS	112 bits + PHY header
ACK	112 bits + PHY header
Payload	8184 bits
Min backoff window	32 slots
Max backoff stage	3
Antenna elements	4

Table 3. SNR vs. data rate.

Threshold (dB)	0	3	5.5	8.5
Data rate (Mbps)	1	2	5.5	11

p_4 : S_k transmits its RTS packet and the transmission is successful. Note that if the RTS packet is faded, there is no corresponding CTS transmission:

$$p_4 = (1-p_f)\tau(1-\tau)(1-\tau+\tau p_f)^{K_a-2}. \quad (19)$$

p_5 : The RTS packet of S_k cannot be received correctly due to collision or fading:

$$p_5 = \tau\left[1-(1-p_f)(1-\tau)(1-\tau+\tau p_f)^{K_a-2}\right]. \quad (20)$$

Let R denote the data rate. In general, R is time-varying due to the time-varying channel conditions, and can be expressed as a function of the instantaneous signal-to-noise ratio (SNR), denoted γ. Then, the average transmission duration is given as

$$\mathbb{E}[T_p] = \int_L \int_\gamma \frac{L}{R(\gamma)} g_{\text{L}}(L) g_\gamma(\gamma) d\gamma dL, \quad (21)$$

where g_{L} and g_γ denote the pdf for the payload L and SNR γ, respectively.

In summary, we have the following result on the saturation throughput per user.

Proposition 1: In an ad hoc network using spatial diversity, the saturation throughput per user is given by

$$U(\rho) = \frac{p_4 \mathbb{E}[L]}{\epsilon p_1 + T_s(p_2+p_4) + T_c(p_3+p_5)}, \quad (22)$$

where $p_i, i = 1, \cdots, 5$, are given in (16)–(20).

We note that the proposed analysis method can yield the same result for system saturation throughput, when it is applied to one BSS case in [9].

D. Numerical Examples

In this section, we investigate the performance of the SD-MAC via numerical examples. Suppose that 4-element antenna arrays are used. We use the single antenna case as a baseline,

Table 4. Saturation throughput vs. number of users.

(The spatial diversity case)

Number of users	10	15	20	30
U (Mbps)	0.330	0.219	0.163	0.107
K_aU (Mbps)	3.30	3.28	3.26	3.21

Table 5. Saturation throughput vs. number of users.

(The single antenna case)

Number of users	10	15	20	30
U (Mbps)	0.138	0.0927	0.0696	0.0465
K_aU (Mbps)	1.38	1.390	1.392	1.395

Table 6. Throughput gain vs. number of users.

Number of users	10	15	20	30
Throughput gain	140%	136%	134%	130%

and define the throughput gain as $\frac{U_m - U_0}{U_0}$, where U_m and U_0 denote the saturation throughput per user corresponding to the multiple antenna case and the single antenna case, respectively. We assume that the users are uniformly distributed. The path loss factor is 2.5. The coverage range is 200 m. The average SNR on the boundary for the single antenna case is 0 dB, and multi-rate transmission is used. The common parameters used in both cases are summarized in Table 2 (see also [20]). Using the practical parameters from D-link, the information-bearing data rate and the SNR (after the processing of spatial diversity) satisfy the relationship as in Table 3.

First, we present the saturation throughput results corresponding to the analytical models. Table 4 depicts the saturation throughput of MIMO ad hoc networks using spatial diversity. We observe that the throughput per user decreases as the number of neighboring users (denoted K_a) involved in contention increases, as expected. For comparison, we also present the saturation throughput of ad hoc networks with single antennas in Table 5.

Table 6 shows that the spatial diversity technique can enhance the throughput significantly in fading channels. Intuitively, due to spatial diversity, the reliability of each link is improved, leading to a higher probability of high-data-rate transmissions. Moreover, we observe that the throughput gain decreases as the the number of users increases. Our intuition is that with multiple antennas, the link is more reliable, and the packet loss due to fading is "dominated" by the packet loss due to collisions. Thus, when more users are involved in contention, the packet loss probability due to contention in the spatial diversity case may increase faster than that in the single antenna case, resulting in a lower throughput gain.

Next, we carry out simulation experiments using an event-driven network simulator—GloMoSim [21]. We have implemented space-time block codes $\mathcal{H}_4$ (see [7] for details) in this simulator. The simulation parameters are listed in Table 7. The nodes are uniformly distributed in an area of (250 m, 250 m). Table 8 presents the saturation throughput for the single antenna case and the spatial diversity case. Table 9 depicts throughput gains with respect to the number of users in the area. We observe that the conclusions derived from theoretic studies can be

Table 7. Simulation parameters for GloMoSim.

Tx power	20 dBm
Path-loss factor	2.5
Rx sensitivity	−91 dBm
Rx threshold	−88 dBm
Rx SINR threshold	0 dB

Table 8. Saturation throughput vs. number of users.

(Single antenna case)

Number of users	10	15	20	30
U (Mbps)	0.0941	0.0660	0.0515	0.0357
K_aU (Mbps)	0.941	0.99	1.03	1.07

(Spatial diversity case)

Number of users	10	15	20	30
U (Mbps)	0.222	0.1407	0.1035	0.066
K_aU (Mbps)	2.22	2.11	2.07	1.98

Table 9. Throughput gain vs. number of users.

Number of users	10	15	20	30
Throughput gain	136%	113%	101%	85%

drawn for the simulation experiments using GloMoSim.

IV. IMPACT OF MIMO MAC ON ROUTING

In the above, we explore SD-MAC design in ad hoc networks. It should be cautioned that an isolated cross-layer strategy may yield unintended system performance, when such a strategy interacts with protocols in other layers. For instance, in [5], the authors show that rate adaptive MAC working with minimum hop routing may lead to poorer performance than fixed high-rate IEEE 802.11 MAC with minimum hop routing. This indicates that a good cross-layer scheme should take into account the interactions across multiple layers. Then, it is natural to ask how the system would perform when the SD-MAC interacts with routing. To answer this question, we extend our cross-layer study to joint consideration of MAC and routing. In particular, we investigate the impact of SD-MAC on routing, and characterize the optimal hop distance in the sense of minimizing the end-to-end delay, by making use of the information from PHY and MAC layers.

In a multi-hop network, the "end-to-end" transport delay is a key performance metric [8]. Roughly speaking, the transport delay consists of the waiting time and the MAC transmission delay, where the MAC transmission delay refers to the sum of the delay due to the contention across users and the packet transmission time. Consider a multi-hop network, where every user uses a given transmission power, and multi-rate adaptation is conducted based on the channel conditions. Let d denote the hop distance, T_d denote the corresponding one-hop delay, and D denote the end-to-end distance a message would travel. Following the giant stepping notion in [8], we consider a large network where each node can find a relay node with a hop distance close to d. Thus, the total delay T_{tot}, can be approximated as [8]

$$T_{tot} = T_d \frac{D}{d}, \tag{23}$$

where $T_d = f(\text{hop distance, rate adaptation, contention})$. Given rate adaption and multi-access strategies, the design of the hop distance is of great importance to minimize the transport delay.

We note that similar problems have been studies in multi-hop ALOHA systems (e.g., [15], [16], and [17]). Worth pointing out is that in ALOHA systems, each user transmits packets in a pre-determined probability, whereas in ad hoc networks with CSMA/CA, carrier sensing is used by each user to regulate its transmission and to mitigate the collision. As mentioned above, in such an ad hoc network, the contention of each user affects the entire network, making the optimal design more challenging.

A. The Optimal Hop Distance

In mobile ad hoc networks, the topology is constantly changing due to user mobility. A key goal of this paper is to optimize the hop distance, in the average sense. Based on [8], we consider the following optimization problem:

$$d^* = \arg\min \left(T_d \frac{D}{d}\right). \tag{24}$$

We study this because the optimal value of d^* can provide insights on how to make use of the gain from the MIMO techniques. For instance, if d^* corresponding to MIMO ad hoc networks is greater than that in the single antenna case, the gain from MIMO channels can be used for longer hop routing. Note that given a fixed transmission power and communication techniques, the coverage range is determined. In practice, the one-hop distance cannot be greater than the coverage range.

We assume that there is a M/M/1 queue at each node (see also [22]). Along the line of Jackson's theorem [22], the traffic arrival rate of node k is given by

$$\lambda_k = \sum_i \beta_{ik} x_i, \tag{25}$$

where x_i is the average transmission rate of node i, and β_{ik} denotes the fraction of packets of node i that go to node k.

For tractability, we consider a homogenous network with heavy traffic. Specifically, the queue of each user is non-empty (a.k.a. saturation conditions [9]). By definition, in a homogeneous network, each node experiences the same statistics. Then, the arrival rate of one node can be expressed as

$$\lambda = \left(\sum_i \beta_{ik}\right)\mu, \tag{26}$$

where μ denotes the average throughput of one user. It follows that the utilization factor $\rho = \lambda/\mu$ is a constant. Thus, the average one-hop delay T_d is given by

$$T_d = \frac{1/\mu}{1-\rho} = aT_h, \tag{27}$$

where $T_h = 1/\mu$ is *one-hop MAC transmission delay*, and $a = 1/(1-\rho)$ is constant. As a result, the optimization problem can be re-written as

$$d^* = \arg\min \left(T_h \frac{D}{d}\right). \tag{28}$$

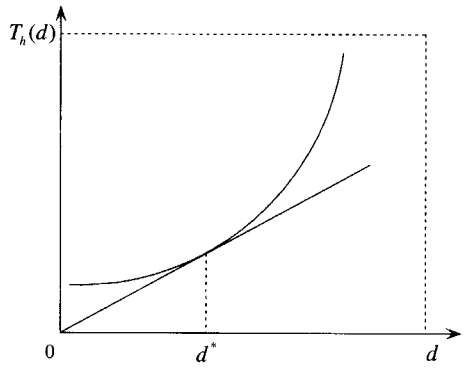

Fig. 2. Optimal hop distance for minimizing delay.

Let B denote the size of one packet. The one-hop transmission delay of one network packet has the form of

$$T_h(d) = \frac{B}{U(d)}. \tag{29}$$

Differentiating $T_h(d)\frac{D}{d}$ with respect to d, we can find that the optimal hop distance d^* satisfies

$$\frac{\partial T_h(d)}{\partial d} = \frac{T_h(d)}{d}. \tag{30}$$

Therefore, we can get the optimal solution d^* by using numerical methods. Similar to the giant stepping notion in [8], the optimal solution is achieved at the point of tangency, as shown in Fig. 2, where the curve depicts a typical trade-off profile between the hop distance and the delay.

Now, the optimal problem boils down to characterizing the average saturation throughput per user. In this case, we apply the results in Section III. Assume that there are K_a users within the coverage of each node. Needless to say, the packet loss probability due to fading is related to the distance between the nodes. For the signal of the desired link, since the hop distance is d, the corresponding packet loss probability q_s is given by $p_f(d)$. Next, we calculate pack loss probability due to fading for the signal from contention nodes. Suppose the contention nodes in the neighborhood are distributed with pdf $f_r(r)$. Thus, the average packet loss probability due to fading, corresponding to the signals from each neighboring contention node can be given as

$$q_n = \int_0^A p_f(r) f_r(r) dr. \tag{31}$$

The probability the RTS packet loss due to the collision can be calculated as

$$\begin{aligned} p_c &= (1-q_s)\Big[1-(1-\tau)\Big((1-\tau)^{K_a-2} \\ &\quad + \binom{K_a-2}{1}(1-\tau)^{K_a-2}\tau q_n + \cdots + (\tau q_n)^{K_a-2}\Big)\Big] \\ &= (1-q_s)\Big[1-(1-\tau)(1-\tau+\tau q_n)^{K_a-2}\Big]. \end{aligned} \tag{32}$$

Therefore, the loss probability of the RTS packet is given by

$$p = p_c + q_s = (1-q_s)\Big[1-(1-\tau+\tau q_n)^{K_a-1}\Big] + q_s. \tag{33}$$

Combining (9) and (33), τ and p can be obtained by numerical methods.

Then, the state probabilities can be expressed as follows:

$$p_1 = (1-\tau)(1-\tau+\tau q_s)(1-\tau+\tau q_n)^{K_a-2}, \tag{34}$$

$$\begin{aligned} p_2 =& (1-\tau)\big[(1-q_s)\tau(1-\tau+\tau q_n)^{K_a-2} + (1-\tau+\tau q_s) \\ & (K_a-2)(1-q_n)\tau(1-\tau+\tau q_n)^{K_a-3}\big], \end{aligned} \tag{35}$$

$$\begin{aligned} p_3 =& (1-\tau)\big\{1-(1-\tau+\tau q_s)(1-\tau+\tau q_n)^{K_a-2} \\ & -\big[(1-q_s)\tau(1-\tau+\tau q_n)^{K_a-2} + (1-\tau+\tau q_s) \\ & (K_a-2)(1-q_n)\tau(1-\tau+\tau q_n)^{K_a-3}\big]\big\} \\ =& (1-\tau)\big\{1-\big[\tau(1-\tau+\tau q_n)^{K_a-2} + (1-\tau+\tau q_s) \\ & (K_a-2)(1-q_n)\tau(1-\tau+\tau q_n)^{K_a-3}\big]\big\}, \end{aligned} \tag{36}$$

$$p_4 = (1-q_s)\tau(1-\tau)(1-\tau+\tau q_n)^{K_a-2}, \tag{37}$$

$$p_5 = \tau\Big[1-(1-q_s)(1-\tau)(1-\tau+\tau q_n)^{K_a-2}\Big]. \tag{38}$$

Then, the average throughput can be derived by plugging the above state probabilities into (22); and the optimal hop distance can be found by using (30).

B. Routing Based on Distance Deviation

To investigate the impact of SD-MAC, we devise a routing scheme that exploits hop distance information. Note that in minimum hop routing, the number of hops is used as a metric, and the routing protocol optimizes the routing tables by choosing the paths with the smallest possible metric. Along the same line, we use the total distance deviation as a performance metric, i.e.,

$$\Delta_D = \sum_i |d_i - d|, \tag{39}$$

where d is the predetermined hop distance, and d_i is the distance of the ith hop. Then, the Bellman-Ford algorithm can be used to optimize the routing by minimizing the above distance deviation metric.

C. Numerical Examples

Now, we present numerical examples to illustrate how to characterize the optimal hop distance. We also study the impact of SD-MAC, rate adaptation strategies, and contention on the hop distance.

The parameters used in the following examples are the same as in Table 2. We assume that the total transmission power of each node is 20 dBm and the path loss factor is 2.5, resulting in a coverage range 200 m for transceivers with signal antennas. The rate adaptation strategy uses the practical parameters from "D-link". The information-bearing data rate and the SNR (after the processing of spatial diversity) have the relationship as in Table 3.

It should be cautioned that the numerical results are based on case studies. Although the proposed method can be applied to

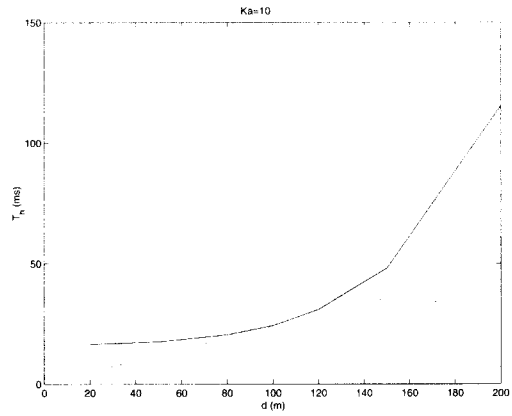

Fig. 3. One-hop transmission delay vs. hop distance (the single antenna case).

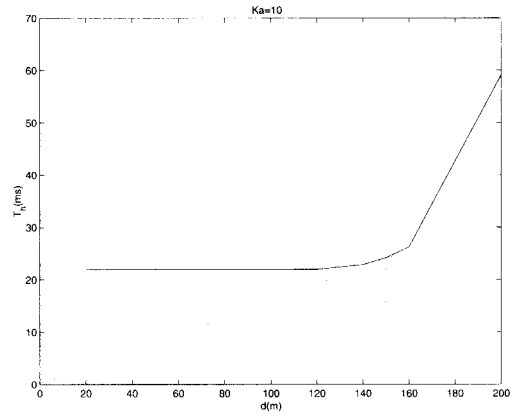

Fig. 4. One-hop transmission delay vs. hop distance (the spatial diversity case).

general homogeneous networks, the absolute value of the optimal hop distance depends on the network topology, the rate adaptation strategy, the node density, and the MAC protocol.

C.1 Impact of SD-MAC

For the sake of comparison, we first examine ad hoc networks with single antennas. Fig. 3 depicts the one-hop transmission delay of each CBR packet with respect to the hop distance, where $K_a = 10$. We observe that the minimum-hop routing using the maximal hop distance together with rate adaptation, or the minimum-hop routing using short-hop with 11 Mbps data rate transmission cannot achieve the best performance. The optimal hop distance minimizing the transmission delay can be found to be 100 m, using the method in Section IV. The corresponding average transmission data rate is 5.66 Mbps.

Next, we examine the trade-off between the delay and the hop distance in ad hoc networks using spatial diversity. Suppose that 4-element antenna arrays are used and the rate adaptation strategy follows Table 3. In Fig. 4, we observe that the optimal lop distance is much larger than the one in the single antenna case, as expected. Intuitively speaking, this is because spatial diversity can improve the link quality greatly. That is to say, for the same data rate, longer hops can be used for the spatial diversity case. Moreover, we note that the reduction in delay is not substantial in the short-hop region; and this is because the transmission strategy does not make full use of the improved link quality

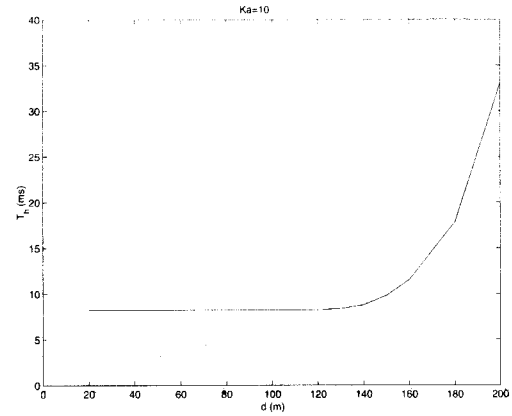

Fig. 5. One-hop transmission delay vs. hop distance (spatial diversity with OAR).

offered by spatial diversity. Recall that in the MAC protocol, the RTS, CTS, ACK, and overhead of DATA are transmitted in the basic data rate 1 Mbps. Under such a strategy, the overhead dominates the improvement from higher rate for data transmissions. We conclude that the gain from spatial diversity can be used to achieve longer hop distances.

C.2 Impact of Rate Control

We now examine the impact of different rate adaptation schemes on the routing. In particular, we first use the opportunistic auto rate (OAR) scheme in the proposed SD-MAC. Suppose that the duration of MAC payload is fixed to be $T_{\text{OAR}} = 8184$ μs. It follows that the payload of one MAC packet is $T_{\text{OAR}}R$, where R is the transmission rate. As expected, the optimal hop distance is achieved at the point of tangency (see Fig. 5). In this case, the optimal hop distance is 140 m. Also, we can see the one-hop transmission delay is reduced significantly. This is because the gain from spatial diversity is also used for achieving higher data rate. Next, we use a rate adaption scheme that allows finer data rates. Specifically, we assume that the transmission data rate can be expressed as (see also [23])

$$R(t) = \alpha C(t),\ 0 < \alpha < 1, \tag{40}$$

where α denotes the efficiency, $C(t)$ is the channel capacity:

$$C(t) = \mathbf{B}\log_2\big(1 + \text{SNR}(t)\big), \tag{41}$$

and $\mathbf{B}$ denotes the bandwidth. Using the parameters in Table 3 from "D-link", we capture the relationship between the practical data rate and the channel capacity, and the coefficient α is given in Table 10. In Fig. 6, it can be seen that this scheme, combined with OAR, can reduce the transmission delay significantly. Our intuition is that when the rate adaptation schemes allow higher data rates, more flexibility is provided for choosing the hop distance and the data rate, leading to better performance. Moreover, we observe that the optimal performance is achieved at the hop distance $d^* = 125$ m, which is shorter than before.

C.3 Impact of Contention

We now investigate the impact of contention on the hop distance. We use the same rate adaptation scheme in the above.

Table 10. SNR vs. coefficient α.

Threshold (dB)	0	3	5.5	8.5
Coefficient α	0.1	0.12	0.23	0.33

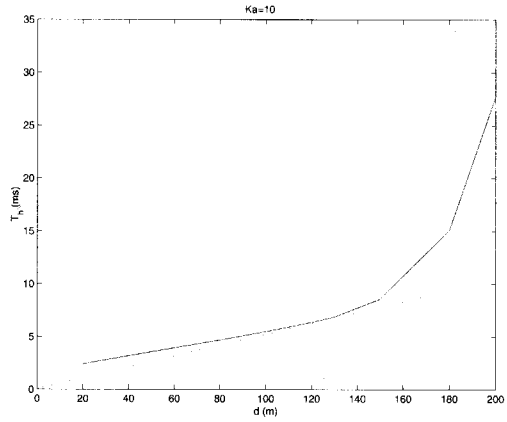

Fig. 6. One-hop transmission delay vs. hop distance (spatial diversity with OAR and finer rates).

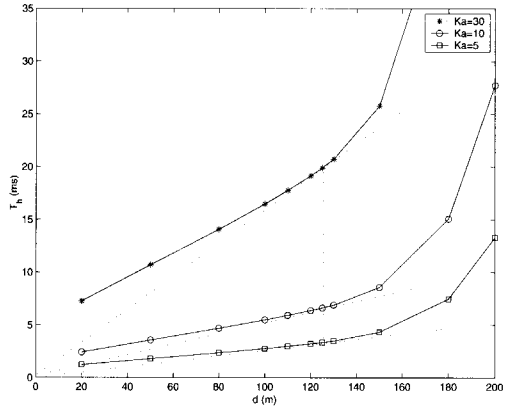

Fig. 7. One-hop transmission delay vs. hop distance (for cases with different node densities).

Fig. 7 depicts the optimal hop distance in the cases with different node densities (where $K_a = \pi A^2 \rho$). An interesting observation is that the optimal hop distance is not sensitive to the node density. We also examine the impact of the node density on the optimal hop distance, under different rate adaptation schemes; and the same observation on the insensitivity also carries over to those cases. Our intuition is that the one-hop transmission delay is approximately proportional to the node density (as shown in Fig. 7), which leads to the same optimal hop distance.

C.4 Routing with Different Hop Distances

Next, we examine the routing with different predetermined hop distances. Particularly, we evaluate the average end-to-end delay and system throughput performance via GloMoSim. For simplicity, we place 100 nodes in a (500 m, 500 m) grid plane, and the distance of every two next nodes is 50 m. Four 15-minute CBR connections are started simultaneously for far-away nodes with the same total distance.

We examine the average end-to-end delay for ad hoc networks with single antennas/spatial diversity. In Table 11, we can see that in the ad hoc networks with single antennas, a hop distance 100 m leads to the best performance. As expected, we also observe that the ad hoc network model with spatial diversity achieves a smaller end-to-end delay. The intuition is that with spatial diversity, the ad hoc network would experience smaller packet loss rate, and therefore the retransmission of RTS packet is reduced. Also, the improved SNR by spatial diversity would lead to a higher data rate. As a result, the end-to-end delay is reduced significantly. In contrast to ad hoc networks with single antennas, in ad hoc networks with spatial diversity, a longer hop distance (i.e., 150 m) yields the best performance. This result corroborates with our theoretical analysis.

Table 11. Average end-to-end delay vs. hop distance.

(The single antenna case)

Hop distance	50	100	150	200
Delay (s)	2.56	0.57	0.90	3.02

(The spatial diversity case)

Hop distance	50	100	150	200
Delay (s)	0.46	0.13	0.11	0.48

We conclude that interaction between SD-MAC and routing has an important impact on the network performance. There exist optimal hop distances that can utilize the gain from the MIMO techniques to minimize the delay. More specifically, the gain from spatial diversity can be used not only to increase the transmission data rate, but also to enlarge the hop distance. Such an optimal hop distance can be found by using the proposed approach above.

V. MAC DESIGN USING DIRECTIONAL ANTENNAS

When the wireless channel has a LOS, directional antennas can yield gains for the desired signals while suppressing the interference. This property allows us to use directional antennas to enhance the performance of the ad hoc networks. For the sake of completeness, we also study ad hoc networks using directional antennas. In particular, we first give a brief review of the directional antenna techniques, and then develop a MAC protocol for ad hoc networks using directional antennas.

A. Directional Antennas

In wireless systems, smart antennas are often used if there exists a LOS. Roughly speaking, smart antennas have three forms: 1) Switch-beam antennas, which consists of switchable narrow beam antennas; 2) smart directional antennas, whose antenna pattern has a fixed shape but the direction of the mainlobe is steerable; and 3) adaptive (pattern) antennas, whose antenna pattern is totally adaptive (see also [13]). We note that the switch-beam antenna can only select the beam on some pre-determined directions, which may incur some loss of performance, whereas the adaptive antenna technique is more complicated to be implemented in mobile terminals. In this paper, we focus on smart directional antennas. The directional antenna technique has two key elements: Direction of arrival (DOA) estimation and directional beamforming. Roughly, if there exists a LOS path, the

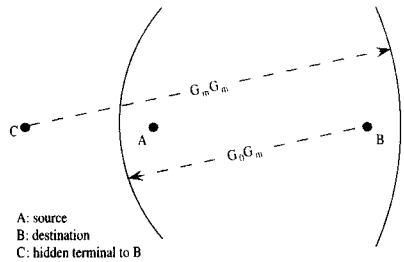

Fig. 8. A hidden terminal problem due to asymmetry in antenna gain.

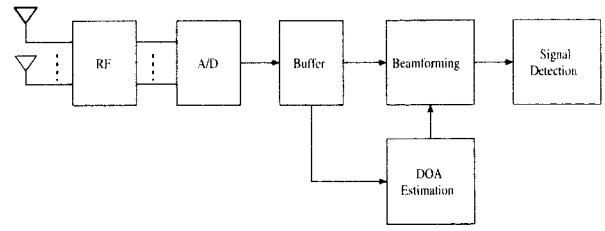

Fig. 9. A block diagram for directional listening.

antenna elements receive replica of the transmitted signal with different delays. Note that the delay is a function of the DOA. By using the difference in the delays, the estimation algorithm (e.g., MUSIC [24]) can detect the DOA accurately. Based on the detected DOA, the smart antenna then chooses a steering vector $\mathbf{w}$ to form a directional antenna pattern to compensate the delays, thereby tuning its direction to the desired user. The received signal with directional beamforming can be expressed as

$$y = \mathbf{w}^{\mathbf{T}}\mathbf{x} + \mathbf{v}, \tag{42}$$

where $\mathbf{x} = [x_1, \cdots, x_M]^T$ denotes the received signal on antenna elements, and $\mathbf{v}$ is the noise. The directional antenna array can be characterized by the antenna gain pattern $G(\theta)$.

Based on the reciprocity theorem [25], the transmit antennas have the reciprocal behavior as the receive antennas, and thus the above results are also applicable to transmit antennas. That is to say, with the same steering vector $\mathbf{w}$, the transmit and receive antennas would have the same antenna pattern.

B. MAC Protocol Using Directional Antennas

Recently, there has been an increasing interest in ad hoc networks with directional antennas (e.g., [11], [12], [14], and the references therein). Recent works [11], [12] assume ideal beamforming and *omnidirectional listening*. In practice, however, the sidelobes may not be negligible. Moreover, since different antenna patterns lead to different antenna gains, the asymmetry in directional transmission/reception and omnidirectional listening, may result in the hidden terminal problem [11], [12]. For example, assume in Fig. 8 that node A transmits a directional RTS packet to node B, while node C is idle. Upon receiving RTS packet, node B sends a directional CTS to node A. Then, nodes A and B are engaged in DATA transmission, both using directional antennas with gain G_m. Note the coverage range is determined by both transmit and receive antenna gain. Let G_0 denote the gain of omnidirectional antennas. The total antenna gain taking into account both directional transmission and omnidirectional listening is G_0G_m, smaller than G_m^2 when directional antennas are used for both transmission and reception. Therefore, node C using omnidirectional listening may not detect the directional CTS packet from node B. But, when the DATA packet from node A to node B is in progress, it is likely that the directional RTS from node C (with the directional beam toward node B) can cause a collision, leading to a hidden terminal problem.

We propose to use *directional listening* to resolve the hidden terminal problem. We note that by using the RTS signals as "pilot signals," each node can carry out directional listening via DSP techniques. By directional listening, we mean that each node is capable of listening to multiple nodes simultaneously with corresponding directional antenna patterns. More specifically, the RTS signals received by an antenna array can be stored in a buffer; the digital signal processor (DSP) uses a copy of the data in the buffer to perform the DOA estimation (see [10] and [24]); and with the estimated DOAs and corresponding steering vectors, the DSP processes the data in the buffer again to perform the directional listening (beamforming). Moreover, with recent advances in DSP technologies, the node has the capability of exploiting multiple steering vectors within a packet duration. Therefore, roughly each node can be viewed as listening with smart directional beams pointing to multiple transmissions. A simple diagram is given in Fig. 9. The directional listening can be implemented with such a structure. Since listening, transmission, and reception are all directional and with the same antenna gain pattern, the hidden terminal problem aforementioned is thereby resolved. Indeed, directional listening, together with a general directional antenna model with sidelobes, is incorporated into our MAC protocol; and this is a key feature of the proposed DA-MAC protocol below.

Suppose that each node obtains network connectivity by broadcasting its HELLO packets (see also [26]). Upon receiving such packets, the neighboring nodes can estimate and update the DOA of the broadcasting node. Thus, in the MAC design, we assume that the DOA of the destination node is known to the source node. We now develop a new MAC protocol for ad hoc networks with directional listening, directional transmission, and directional reception. For exploiting the benefits of directional antennas, two tables are used, namely the antenna pattern lookup table and the directional NAV (D-NAV) table. In the antenna pattern lookup table, the antenna gain is listed with respect to the azimuth direction. The D-NAV table consists of the RTS/CTS mode, node index, DOA, the signal power corresponding to each DOA, and NAV derived from the received RTS/CTS packet. The proposed DA-MAC protocol for directional antennas can be outlined as follows.

- *RTS transmission*: The source node, denoted S_k, receives a packet from the upper layer, and obtains the direction of the (next hop) destination node in its connectivity table. Then, the source node S_k performs virtual carrier sensing by using both its D-NAV table and antenna pattern table. Simply put, S_k calculates the effective interference power for the nodes

in the D-NAV as

$$P_e(\theta) = \frac{P_r(\theta)G(\theta - \theta^r_{kk})}{G_m}, \tag{43}$$

where $P_r(\theta)$ is the received power of RTS/CTS in the DOA (denoted θ) by using directional listening, $G(\cdot)$ is the receive antenna pattern, θ^r_{kk} denotes the angle of the mainlobe center, and G_m is the gain of the mainlobe. If for the desired direction, the corresponding $P_e(\theta)$ is below the threshold, the directional channel is viewed idle in the virtual carrier sensing. Then, the source node forms a narrow-beam antenna pattern, and performs physical carrier sensing. If the power of received interference is below the threshold for a period of DIFS, the channel is determined to be available for transmission, and the directional RTS packet is transmitted to the (next hop) destination, denoted D_k. Otherwise, the user S_k needs to backoff a random period and defer its transmission in this direction. In particular, the user continues directional carrier sensing, and counts down the backoff counter only if the channel is idle. When the backoff counter becomes zero, the packet is sent out immediately.

- *RTS/CTS listening*: All idle nodes in the neighborhood overhear the RTS/CTS packets directionally by using smart antenna techniques, and then update their D-NAV tables.
- *RTS reception and CTS transmission*: The destination node D_k overhears the RTS packet using directional reception beamforming. Upon receiving the RTS packet correctly, D_k conducts virtual carrier sensing as done for the *RTS transmission*. If the channel is viewed idle in virtual carrier sensing, D_k forms a directional beam and performs physical carrier sensing. If the channel is idle for a duration SIFS, the node transmits the directional CTS packet to S_k. If the channel is busy, the CTS transmission is cancelled.
- *CTS reception and DATA transmission*: After the RTS transmission, S_k forms a directional receive antenna pattern and waits for the CTS packet. If S_k receives the CTS packet, it performs virtual carrier sensing and physical carrier sensing sequentially. If the channel is idle for a duration of SIFS, the DATA packet is then transmitted directionally. If the CTS packet does not arrive within a predetermined time-out window, S_k will resend the RTS packet.
- *DATA reception and ACK transmission*: After sending out the CTS packet, D_k moves to the DATA reception phase. When the DATA packet is received, D_k confirms the reception by sending a ACK packet to S_k directionally.

In a nutshell, we incorporate directional listening into the MAC design to resolve the hidden terminal problem. Furthermore, the proposed DA-MAC protocol uses a general antenna pattern model with sidelobes, and makes use of directional listening, directional transmission, and directional reception. Clearly, the DA-MAC protocol is tailored to enhance the spatial reuse.

C. Saturation Throughput: The Directional Antenna Case

Suppose that idea beamforming is achieved, and the directional antenna with beamwidth Δ is used from both transmission and reception. Let K_ρ denote the number of mobile stations within the coverage area of one station. In an ad hoc network with the coverage range d and the node density ρ, K_ρ can be approximated as

$$K_\rho = \frac{\Delta}{2\pi}\pi d^2 \rho. \tag{44}$$

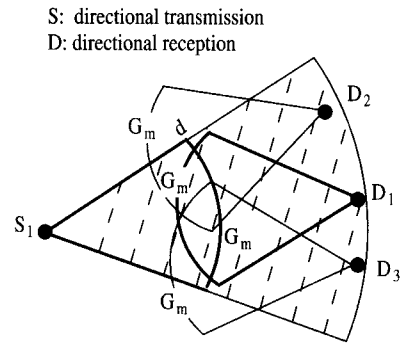

Fig. 10. A diagram of coverage area in ad hoc networks with directional antennas.

Note that the coverage range d is determined by both directional transmission gain and directional reception gain, as depicted in Fig. 10. Moreover, we assume that node S_k knows the address and direction of its destination node, but does not have knowledge about the behavior of the other nodes. Statistically speaking, node S_k just "sees" its neighbors transmit in each direction with equal probability.

We note that the transmission probability τ and the packet loss probability p follow the relationship as in (9). Moreover, in the context above, if S_i is within the reception coverage of some other user, S_i would transmit in the direction to that user with probability $\frac{\Delta}{2\pi}\tau$. Then, the collision probability p can be expressed as

$$p = 1 - (1-\tau)(1 - \frac{\Delta}{2\pi}\tau)^{K_\rho - 2}. \tag{45}$$

Therefore, τ and p can be derived by solving the (9) and (45).

In the following, we derive the saturation throughput for the directional antenna case. Note that the probabilities p_1, p_2, and p_3 describe the states overheard by the S_k using directional listening, and p_4 and p_5 denote the states that the RTS packet of S_k is transmitted.

$$p_1 = (1-\tau)(1 - \frac{\Delta}{2\pi}\tau)^{K_\rho - 1}, \tag{46}$$

$$p_2 = (1-\tau)(K_\rho - 1)\frac{\Delta}{2\pi}\tau(1 - \frac{\Delta}{2\pi}\tau)^{K_\rho - 2}, \tag{47}$$

$$p_3 = (1-\tau)\left[1 - \left(1 - \tfrac{\Delta}{2\pi}\tau\right)^{K_\rho - 1} - (K_\rho - 1)\tfrac{\Delta}{2\pi}\tau\left(1 - \tfrac{\Delta}{2\pi}\tau\right)^{K_\rho - 2}\right], \tag{48}$$

$$p_4 = \tau(1-\tau)(1 - \frac{\Delta}{2\pi}\tau)^{K_\rho - 2}, \tag{49}$$

$$p_5 = \tau\left[1 - (1-\tau)(1 - \frac{\Delta}{2\pi}\tau)^{K_\rho - 2}\right]. \tag{50}$$

Moreover, the durations T_s and T_c have the forms shown in (11) and (12), while the average transmission duration is expressed as

$$\mathbb{E}[T_p] = \frac{\mathbb{E}[L]}{R}, \tag{51}$$

where R is the transmission data rate. Then, the saturation throughput per user can be calculated by using (10).

Note that similar methodology for characterizing the optimal hop distance can be also carried out in ad hoc networks using directional antennas. But, it is beyond the scope of the paper.

D. Numerical Examples

In the following, we examine the performance of the proposed DA-MAC. Note that with directional antennas, the nodes can achieve power gains. That is, using the same transmission power, each node can have a greater coverage range. This can have impact on both connectivity and routing. For instance, the power gain can be used to implement longer hop transmission/routing, and yield further improvement. Since we focus on the MAC design exploiting spatial reuse, such impact on upper layers is beyond the scope of this paper. Thus, in this example, we allow the nodes with antenna arrays to tune the transmission power, thereby having the same coverage range as that with omnidirectional antennas [12]. We assume that 4-element antenna arrays are used and each antenna array has a directional antenna pattern with $\Delta = \pi/2$ approximately. Then, if there are 20 nodes in a neighboring (circle) area, on average 5 nodes are within the coverage area of a directional antenna. Since the channel has LOS only and is fixed over time, we assume a fixed transmission rate 1 Mbps. Table 12 depicts the saturation throughput per user with respect to the number of neighboring nodes. It can be seen that as the number of users increases, the saturation throughput per user decreases. That is, the higher the node density, the lower saturation throughput each user has. It is because that when the node density increases, more nodes are involved in the channel contention. As a result, each node achieves a lower throughput. Table 13 describes the throughput gain with respect to the number of neighboring nodes. We observe that with 4-element directional antennas, the ad hoc networks can yield a throughput gain around 10-fold. Our intuition is that by using directional antennas at both transmitters and receivers, the directional antenna technique can increase the spatial reuse, thereby improving the system throughput significantly.

Worth pointing out is that the above numerical results are derived by the analytical methods above, based on the ideal directional antenna model: $\Delta = \pi/2$ and the antenna gain for sidelobes is 0. In practice, the beamwidth is determined by the antenna pattern design algorithms [25]. Given the number of antennas, the beamwidth (of the mainlobe) Δ, the mainlobe antenna gain, and the sidelobe antenna gain are correlated. Roughly speaking, there is always a trade-off between the beamwidth and the antenna gain. The narrower the beamwidth, the smaller the gain difference between the mainlobe and the sidelobes; and vice versa. To make the interference from the sidelobes negligible, the antenna gain difference should be large, dictating a wider beam, (possibly $\Delta > \pi/2$ for 4-element antennas). In such cases, the system would achieve smaller throughput gains than in the ideal case above.

It should be emphasized that the above results for the spatial diversity case and the directional antenna case are for different wireless channel models (so they are not comparable). When there is i.i.d. time-varying fading, the spatial diversity can combat fading and improve the link quality, whereas the directional antennas would not work well. In contrast, when there is a LOS, the channel is more reliable. Thus, the directional antennas can exploit spatial reuse to improve the system throughput.

VI. CONCLUSIONS

In this paper, we explore the utility of multiple-antenna techniques for MAC design and routing in mobile ad hoc networks. We first examine the impact of spatial diversity on the MAC design, and devise the corresponding MAC protocol, namely SD-MAC. Then, we develop analytical methods to characterize the saturation throughput for ad hoc networks using MIMO MAC. The proposed analytical methods take into account the multi-rate transmissions offered by spatial diversity, fading, and contention, and is applicable to multi-hop ad hoc networks. Furthermore, we study joint design of MIMO MAC and routing. We characterize the optimal hop distance in a large networks. For completeness, we also study MAC design using directional antennas, when the channel has a strong LOS component. We demonstrate the utility of directional listening and incorporate it into the MAC protocol. The numerical results show that the spatial diversity technique and the directional antenna technique can enhance the performance of ad hoc networks significantly.

There are many problems deserving further investigation. For example, we observe that it is difficult to achieve the spatial multiplexing gain in the interference-limited scenarios. But, if one MAC protocol could mitigate the interference effectively, spatial multiplexing might yield significant gains. It is of much interest to explore such a protocol. Moreover, the use of directional antennas is based on the assumption of a strong LOS component. When the LOS component is insignificant, the antenna pattern becomes inaccurate in representing the spatial energy distribution. That is to say, in this case, the spatial footprint of radio energy can be quite different in specific directions. It remains open to characterize a reasonable threshold that can be used to distinguish the environments where directional antennas can work well.

APPDENDIX

Saturation Throughput for Omnidirectional Antenna Case

Suppose that there are K users in a BSS, each with an omnidirectional antenna. We first investigate the states experienced by one user, and derive the probabilities $p_i, i = 1, \cdots, 5$, defined before. Note that in a BSS, each user can hear all other users. The probabilities are given as

$$p_1 = (1-\tau)(1-\tau)^{K-1}, \tag{52}$$

$$p_2 = (1-\tau)(K-1)\tau(1-\tau)^{K-2}, \tag{53}$$

Table 12. Saturation throughput per user vs. number of users: The directional antenna case (for the LOS channel model).

(Omnidirectional antenna case)

Number of users	20	28	36	44	60
U (Mbps)	0.0491	0.0350	0.0271	0.0221	0.016

(Directional antenna case)

Number of users	20	28	36	44	60
U (Mbps)	0.4896	0.3928	0.3279	0.2808	0.2191

Table 13. Throughput gain vs. number of users (for the LOS channel model).

Number of users	20	28	36	44	60
Throughput gain	997%	1120%	1210%	1270%	1370%

$$p_3 = (1-\tau)\left[1-(1-\tau)^{K-1}-(K-1)\tau(1-\tau)^{K-2}\right], \quad (54)$$

$$p_4 = \tau(1-\tau)^{K-1}, \quad (55)$$

$$p_5 = \tau\left(1-(1-\tau)^{K-1}\right). \quad (56)$$

Moreover, we have $T_1 = \epsilon$, $T_2 = T_4 = T_s$, and $T_3 = T_5 = T_c$. Then, we can calculate the average throughput of one user by plugging $\{p_i, T_i\}, i = 1, \cdots, 5$, into (10), i.e.,

$$\begin{aligned} U = {} & \tau(1-\tau)^{K-1}\mathbb{E}[L] \\ & \left[(1-\tau)^{K_\varepsilon} + K\tau(1-\tau)^{K-1}T_s \right. \\ & \left. +\{1-(1-\tau)^K - K\tau(1-\tau)^{K-1}\}T_c\right]^{-1}. \end{aligned} \quad (57)$$

Since each user statistically has the same performance and its corresponding throughput does not overlap with others, the system saturation throughput U_s is given by

$$\begin{aligned} U_s = \sum_{i=1}^{K} U_i &= \left(K\tau(1-\tau)^{K-1}\mathbb{E}[L]\right) \\ &\times \left[(1-\tau)^{K_\varepsilon} + K\tau(1-\tau)^{K-1}T_s \right. \\ &\left. + \left\{1-(1-\tau)^K - K\tau(1-\tau)^{K-1}\right\}T_c\right]^{-1} \\ &= p_{tr}p_s\mathbb{E}[L] \\ &\times \left\{(1-p_{tr})\varepsilon + p_{tr}p_sT_s + p_{tr}(1-p_s)T_c\right\}^{-1}. \end{aligned} \quad (58)$$

That is, the proposed analysis method yields the same results in [9].

REFERENCES

[1] G. J. Foschini and M. J. Gans, "On limits of wireless communications in a fading environment when using multiple antennas," *Wireless Pers. Commun.*, vol. 6, no. 3, pp. 311–335, Mar. 1998.

[2] I. E. Telatar, "Capacity of multi-antenna gaussian channels," *European Trans. Telecommun.*, vol. 10, pp. 585–595, Dec. 1999.

[3] H. Bölcskei, "Fundamental performance tradeoffs in coherent MIMO signaling," *Private Commun.*, 2003.

[4] L. Zheng and D. N. Tse, "Diversity and multiplexing: A fundamental tradeoff in multiple-antenna channels," *IEEE Trans. Inform. Theory*, vol. 49, pp. 1073–1096, May 2003.

[5] S. Alamouti, "A simple transmit diversity technique for wireless communications," *IEEE J. Select. Areas Commun.*, vol. 16, pp. 1451–1458, Oct. 1998.

[6] A. Narula, M. D. Trott, and G. W. Wornell, "Performance limits of coded diversity methods for transmitter antenna arrays," *IEEE Trans. Inform. Theory*, vol. 45, pp. 2418–2433, Nov. 1999.

[7] V. Tarokh, N. Seshadri, and A. R. Calderbank, "Space-time codes for high data rate wireless communication: Performance criterion and code construction," *IEEE Trans. Inform. Theory*, vol. 44, no. 2, pp. 744–765, Mar. 1998.

[8] L. Kleinrock, "On some principles of nomadic computing and multi-access communications," *IEEE Commun. Mag.*, pp. 46–50, July 2000.

[9] G. Bianchi, "Performance analysis of the IEEE 802.11 distributed coordination function," *IEEE J. Select. Areas Commun.*, vol. 18, pp. 535–547, Mar. 2000.

[10] J. C. Liberti and T. S. Rappaport, *Smart Antennas for Wireless Communications*, Prentice Hall, 1999.

[11] R. R. Choudhary *et al.*, "Using directional antennas for media access control in ad-hoc networks," in *Proc. IEEE/ACM MobiCom 2002*, 2002.

[12] T. Korakis, G. Jakllari, and L. Tassiulas, "A MAC protocol for full exploitation of directional antennas in adhoc wireless networks," in *Proc. IEEE/ACM MobiHoc 2003*, June 2003, pp. 98–107.

[13] K. Sundaresan *et al.*, "A fair medium access control protocol for ad-hoc networks with MIMO links," in *Proc. IEEE/ACM INFOCOM 2004*, Mar. 2004.

[14] L. Bao and J. Garcia-Luna-Aceves, "Transmission scheduling in ad hoc networks with directional antennas," in *Proc. IEEE/ACM MobiCom 2002*, Sept. 2002.

[15] L. Kleinrock and J. Silvester, "Optimum transmission radii for packet radio networks or why six is a magic number," in *Proc. IEEE National Telecommun. Conf.*, Dec. 1978.

[16] T. Hou and V. Li, "Transmission range control in multihop packet radio networks," *IEEE Trans. Commun.*, pp. 38–44, Jan. 1986.

[17] V. Wong and C. Leung, "Transmission strategies in multihop mobile packet radio networks," in *Proc. Canadian Conf. Electrical and Computer Engineering*, Sept. 1993, pp. 1004–1008.

[18] V. Kawadia and P. R. Kumar, "A cautionary perspective on cross layer design," *preprint*, 2003.

[19] D. Gesbert *et al.*, "From theory to practice: An overview of MIMO space-time coded wireless systems," *IEEE J. Select. Areas Commun.*, vol. 21, pp. 281–302, Apr. 2003.

[20] IEEE Standard, "Wireless LAN medium access control (MAC) and physical layer (PHY) specifications," Nov. 1997.

[21] UCLA, "http://pcl.cs.ucla.edu/projects/glomosim/," 2003.

[22] D. Bertsekas and R. Gallager, *Data Networks*, Prentice Hall, 2000.

[23] E. Uysal-Biyikoglu, B. Prabhakar, and A. E. Gamal, "Energy-efficient packet transmission over a wireless link," *IEEE Trans. Networking*, no. 4, pp. 487–499, Aug. 2002.

[24] R. Schmidt, "Multiple emitter location and signal parameter estimation," *IEEE Trans. Antennas Propagat.*, vol. 34, pp. 276–280, 1986.

[25] C. Balanis, *Antenna Theory Analysis and Design*, New York: John Wiley & Sons Inc., 1997.

[26] A. Muqattash and M. Krunz, "Power controlled dual channel (PCDC) medium access protocol for wireless ad hoc networks," in *Proc. IEEE INFOCOM 2003*, Apr. 2003.

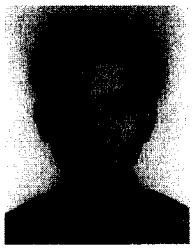

Ming Hu received his Ph.D. degree from the Department of Electrical Engineering at Arizona State University in Aug. 2004. He obtained his B.S. and M.S. degrees in Electronic Engineering from Tsinghua University, Beijing, China, in 1997 and 2000, respectively. Currently, he is a Design Engineer in Nokia Mobile Phones, San Diego, CA. His research interests include wireless networks, wireless data communications, cross-layer design, scheduling, and multiple antenna techniques.

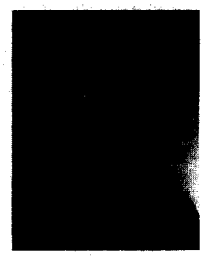

Junshan Zhang received his Ph.D. degree from the School of Electrical and Computer Engineering at Purdue University in 2000. He joined the Department of Electrical Engineering at Arizona State University in Aug. 2000, where he is currently an Assistant Professor.

His research interests fall in the general area of wireless networks, spanning from the networking layer to the physical layer. His current research focusses on fundamental problems in cellular networks, wireless LANs, and mobile ad hoc networks, including cross-layer optimization and design, scheduling, resource management, and network information theory.

Dr. Zhang received a NSF CAREER award in 2003 and the Outstanding Research Award from the IEEE Phoenix Section in 2003. He was chair of the IEEE Communications and Signal Processing Phoenix Chapter from Jan. 2001 to Dec. 2003. He has served as a member of the technical program committees of INFOCOM, GLOBECOM, ICC, MOBIHOC, and SPIE ITCOM. He has served as an Associate Editor for IEEE Transactions on Wireless Communications since 2004.